This is a repository copy of *Quantitative analysis of complex amino acids and RGD peptides by X-ray photoelectron spectroscopy (XPS)*.

White Rose Research Online URL for this paper:
http://eprints.whiterose.ac.uk/84918/

Version: Accepted Version

Quantitative Analysis of Complex Amino Acids and RGD Peptides by X-ray Photoelectron Spectroscopy (XPS)

Joanna S. Stevens,[1] Alba C. de Luca,[2,3] Michalis Pelendritis,[1] Giorgio Terenghi,[2]
Sandra Downes,[3] Sven L. M. Schroeder[1,4] *

[1]School of Chemical Engineering and Analytical Science, The University of Manchester, Oxford Road, Manchester, M13 9PL, UK

[2]Blond McIndoe Laboratories, School of Biomedicine, The University of Manchester, Manchester Academic Health Science Centre, Oxford Road, Manchester M13 9PT, United Kingdom

[3]School of Materials, The University of Manchester, Grosvenor Street, Manchester M13 9PL, United Kingdom

[4]School of Chemistry, The University of Manchester, Brunswick Street, Manchester, M13 9PL, UK

Email: s.schroeder@manchester.ac.uk

*Sven L.M. Schroeder: Tel. +44-161-306 4502; Fax: +44-161-306 8867

Abstract

The C 1s, N 1s, and O 1s core level binding energies of the functional groups in amino acids (glycine, aspartic acid, glutamic acid, arginine, and histidine) with varied side-chains and cell-binding RGD-based peptides have been determined and characterized by XPS with a monochromatic Al K_α source. The zwitterionic nature of the amino acids in the solid state is unequivocally evident from the N 1s signals of the protonated amine groups and the C 1s signature of carboxylate groups. Significant adventitious carbon contamination is evident for all samples but can be quantitatively accounted for. No intrinsic differences in the XP spectra are evident between two polymorphs (α and γ) of glycine, indicating that the crystallographic differences have a minor influence on the core level binding energies for this system. The two nitrogen centers in the imidazole group of histidine exhibit an N 1s binding energy shift that is in line with previously reported data for theophylline and aqueous imidazole solutions, while the nitrogen and carbon chemical shifts reflect the unusual guanidinium chemical environment in arginine. It is shown that the complex envelopes of C 1s and O 1s photoemission spectra for short-chain peptides can be analyzed quantitatively by reference to the less complex XP spectra of the constituent amino acids, provided the peptides are of high enough purity. The distinctive N 1s photoemission from the amide linkages provides an indicator of peptide formation even in the presence of common impurities, and variations in the relative intensities of N 1s were found to be diagnostic for each of the three peptides investigated (RGD, RGDS, and RGDSC).

Keywords

XPS, peptide, polymorph, RGD, glycine, biomaterials

Introduction

Peptide-functionalizedsurfaces are a widely explored strategy towardsbiomaterials with enhanced or specific cell binding properties.[1-3] RGD (Arg-Gly-Asp) peptides in particular are well known to promote cell binding and have therefore been the object of numerous investigations in biomaterials science.[1,4-9]It has been shown that X-ray photoelectron spectroscopy (XPS) can distinguish proteins from other groups of biomolecules such as polysaccharides and lipids through the spectral contrast arising from differences in elemental composition and characteristic functional groups [10,11] Indeed, XPS has been used to characterize RGD-modified surfaces.[12-16] We have recently examined Schwann cell response on the surfaces of poly-ε-caprolactone (PCL) substrates covered with RGD and the pentapeptide RGDSC (Arg-Gly-Asp-Ser-Cys).[13] Quantitative XPS allowed us to follow the immobilization surface chemistry by reference to XPS data of the solid bulk forms of the peptides and of the constituent amino acids of RGD. Core level spectra organic compounds also allow the identification of the presence of protonated and hydrogen-bonded nitrogen groups.[17-22] For amino acids, protonated amino groups reflect the well-known[23-32] zwitterionic state of the molecules in their crystalline form as opposed to the neutral gas phase form. More recent investigations of the amino acids lysine[33,34] and glycine[35,36] as well as studies of the solid forms of pharmaceutical materials[19,20,20-22] have confirmed the ability of XPS to unequivocally determine the presence of protonated Brønsted acceptors.

XPS investigations of amino acids go back as far as the earliest days of photoelectron spectroscopy,[17,37-39] but while there is a recent set of gas phase photoemission and soft X-ray absorption data for several amino acids and some homo-dipeptides,[40-46] high resolution solid state reference data are scarce. We therefore present here our body of quantitative XPS data obtained for the solid forms of the five amino acids and RGD-peptides presented in Figure 1, investigating the zwitterionic nature and varied side-chain groups of the amino acids and drawing attention to the potential for the analysis of oligopeptides as well as potential limitations arising from sample purities. Alongside the amino acids constituting RGD we include data for glutamic acid (Glu), which is a CH_2-homologue to Asp, and of histidine (His), which presents an opportunity to independently verify the N 1s binding energies in its imidazole ring. These N 1s binding energies are of current interest in the context of fundamental investigations with core level spectroscopy of imidazole and its aqueous solutions.[47-50] The results of the measurements reported in this paper underline the ability of XPS to reliably identify the location of protonation in the zwitterions and to distinguish incisively between the various studied amino acids, especially through the presence of photoemission features from functional groups in the more complex amino acid side-chains, whilst the amide signal provides an indicator of peptide formation. The availability of such reference data should aid other researchers in the field, particularly in the interpretation of results of surface functionalization experiments.

Experimental Section

Starting materials

All amino acids except γ-glycine were obtained from Sigma-Aldrich, UK: aspartic (Asp) and glutamic (Glu) acids with >99.5% purity, α-glycine (Gly) and histidine with >99%, and arginine (Arg) with >98%. The

tripeptide RGD (>97% by HPLC)[51] and the tetrapeptide RGDS (>95%) were obtained from Sigma-Aldrich (Dorset, UK), and the pentapeptide RGDSC (96.78 %) from Biomatik Corporation (Cambridge, Canada).

Crystallization of γ-glycine

A mixture of 17.5 g (233 mmol, 1 eq.) of α-glycine and 0.9 g (8.65 mmol, 0.037 eq.) of malonic acid was added to 50 ml of water, heated to 70°C until completely dissolved, then left to cool to 20°C. Continuous stirring throughout the experiment led to non-uniformly shaped crystals and the presence of some α-glycine. Stirring was therefore only performed at the beginning and for a couple of minutes before the end of the crystallization process in order to get larger, more uniformly shaped crystals. When the mixture was completely dissolved, a large γ-glycine crystal (from the previous crystallization) was crushed and introduced in the solution to create nucleation sites for crystal growth (crystal seeding). After the solution had cooled to 20°C, it was stirred until precipitation was observed, then left to settle before filtration. Formation of γ-glycine was confirmed by microscopy (large, rod-like crystals) and comparison of X-ray powder diffraction (XRPD) patterns to single crystal data.[25,26]

X-ray Photoelectron Spectroscopy (XPS)

XP spectra were recorded with a Kratos Axis Ultra instrument employing a monochromatic Al K_α source (1486.69 eV), a hemispherical analyzer with an electrostatic lens system, charge neutralization, and a delay line detector (DLD). Samples were fixed using double-sided tape. Experiments were performed while operating the X-ray source with a power of 180 W (15 kV and 12 mA), with the pressure below 10^{-8} mbar during analysis. The instrument was operated in CAE (constant analysis energy) mode, with a pass energy of 20 eV for high resolution scans of the photoemission from individual core levels, with a calibrated intensity/energy response and transmission function.[52] Surveys were measured in steps of 0.25 eV with 300 ms dwell time per data point. Nitrogen, carbon, and oxygen 1s high resolution spectra were measured within the spectral range of interest (ca. ± 20 eV around the core level emission peaks) with 0.1 eV steps and 300-1000 ms dwell time per data point. Repeats were carried out to check for radiation damage.

Analysis of the data was carried out with CasaXPS software.[53] A linear background was used in curve-fitting (minimizing χ^2)[53,54] along with a GL(30) lineshape (70% Gaussian, 30% Lorentzian using the Gaussian/Lorentzian product form) for the C 1s and N 1s spectra. An exponential tail GL(55)T(2) lineshape[52,53] was used for fitting the O 1s, spectra as there appeared to be some intrinsic asymmetry toward higher binding energy (BE). Samples were referenced to the C 1s emission by adventitious hydrocarbon contamination at 285 eV.[52,54]

Peak widths (FWHMs) were not fixed, to account for variation between different chemical states. Where the presence of multiple overlapping peaks was evident from the data the FWHM values were allowed to vary within constraints (FWHM ranges of 1.1 - 1.5 eV) that appeared plausible in view of the instrument resolution and previously observed data.[52] Peak fitting for the more complex carbon and oxygen 1s spectra started from intensities reflecting the expected stoichiometric ratios for the chemical environments within the chemical

3

structures (Figure 1), letting the C 1s C–C peak component vary in intensity to allow for differing levels of hydrocarbon contamination. Finally, the area ratios of all peaks were allowed to relax to allow for the possibility of non-stoichiometry.[55] All C 1s peak area ratios are given in the Supplementary Information. The peak intensity attributed to adventitious hydrocarbon contamination in the C 1s spectra was subtracted from the elemental composition values obtained from the survey spectra to give the corrected values.[52] Repeatability of the peak positions was ±0.1 eV, while repeatability for the elemental composition values was within ±1.0%. Throughout this paper, when molecular formula fragments are reported the atom of interest is indicated by being underlined where there is possible ambiguity.

Results and Discussion

N 1s XPS

Glycine has a single nitrogen atom in its structure (Figure 1) giving rise to a single photoemission signal at 401.4 eV for both the α- and γ-polymorphic forms (Figure 2a, Table 1). This value is in the range for protonated nitrogen (NH_3^+),[20] in line with the zwitterionic nature of crystalline glycine.[23-26] Aspartic acid and glutamic acid also only have a single α-nitrogen atom and are zwitterionic,[27,28] leading to photoemission signals at 401.6 eV and 401.5 eV respectively (Figures 2b and 2c, Table 1).

Histidine has a side-chain containing an imidazole group (Figure 1), resulting in a total of three nitrogen atoms in the molecule. We previously determined the N 1s binding energies of nitrogen centers in chemically analogous positions in theophylline, in which they are conjugated with additional electron-withdrawing groups, resulting in N 1s binding energies (BEs) of 399.6 eV for the C=N nitrogen and of 401.0 eV for C–NH.[18] The imidazole ring in histidine is not conjugated to electron-withdrawing groups and hence exhibits lower N 1s BEs, at 398.8 eV for C=N and at 400.4 eV for C–NH (Figure 2d, Table 1), in good agreement with the BE shift in aqueous imidazole solutions.[47,56] The third N 1s peak of histidine at 401.4 eV (Figure 2d, Table 1) is again indicative of the zwitterionic, protonated α-amine nitrogen,[29,30] in line with the data for glycine, aspartic, and glutamic acid.

In the zwitterionic form of arginine, the positive charge is delocalized on the side-chain guanidine group (Figure 1), and not located at the usual α-amine position.[32] The N 1s spectrum therefore exhibits two peak components at 399.2 and 400.0 eV, with an intensity peak area ratio of 1:3.[17] The peak at 400.0 eV is representative of the three nitrogen atoms with the delocalized positive charge, while that at 399.2 eV arises from the amine α-C–N nitrogen (Figure 2e, Table 1).

The peptide RGD (its structure is shown Figure 1) has two amide N–C=O linkages that lead to photoemission at 400.1 eV (Figure 3a, Table 1), along with a small peak at higher binding energy, at 401.6 eV, arising from the protonated arginine α-NH_3^+ of the N-terminus. This second protonation occurs due to Brønsted donation from the second carboxylic acid group of aspartic acid.[57] As in arginine, additional contributions to the 400.1 eV peak of RGD arise from the guanidine group (Table 1).

The addition of serine in the tetrapeptide RGDS increases the amide intensity relative to that of the α-NH_3^+ nitrogen photoemission peak (Figure 3), increasing the peak area ratio (Table 1) through the presence of an additional peptide bond. Similarly, the pentapeptide RGDSC incorporates cysteine at the C-terminus, further

4

increasing the amide intensity and peak area ratio (Figure 3, Table 1), as well as giving rise to a sulfur 2p photoemission signal at 164.1 eV.

C 1s and survey XPS

The two carbon atoms of glycine give rise to two photoemission signals from their different chemical environments (Table 2). In α-glycine, the $\underline{C}-NH_3^+$ peak arises at 286.4 eV and COO^- at 288.5 eV (Figure 4a, Table 3). The BE positions are identical to within 0.1 eV for the γ-polymorph. The lowest BE C 1s peak component at 285 eV arises from adventitious hydrocarbon contamination ($\underline{C}-C$),[54] and is of greater intensity for the γ-polymorph (Figure 4a, inset). This could indicate surface impurities introduced during the preparation of the γ-form, likely some of the malonic acid added to the crystallization process.After removal of the adventitious hydrocarbon contribution from the elemental composition,[52] there is good agreement between the experimentally observed and the expected stoichiometry values of the amino acids (Table 4).

Five peak components are fit in the C 1s spectrum of aspartic acid, with the lowest BE peak at 285 eV again from adventitious hydrocarbon contamination (Figure 4b, Table 3). The four chemical environments of carbon within the aspartic acid molecule (Table 2) give rise to four peaks: $\underline{C}-COOH$ at 285.4 eV, $\underline{C}-NH_3^+$ at 286.6 eV, COO^- at 288.5, and the side-chain COOH at 289.4 eV. The carboxylate COO^- signal is at slightly lower BE than for the carboxylic acid (COOH), in accordance with the higher electron density at carbon for the carboxylate.[17,58,59] Glutamic acid has the same carbon environments as aspartic acid, with the addition of a side-chain methylene $\underline{C}-C$. In line with this, all C 1s peak components occur within 0.2 eV of those in aspartic acid (Figure 4c, Table 3).

The carbons of histidine (Table 2) give rise to five peak components of increasing electronegativity, with $\underline{C}-C$ at 285.0 eV, $C=\underline{C}-N$ at 285.6 eV, $\underline{C}-NH_3^+$ at 286.2 eV, $N=\underline{C}-NH$ at 286.7 eV, and COO^- at 288.3 eV (Figure 4d, Table 3). As with nitrogen, the imidazole ring carbon signals are slightly shifted to lower BEs compared to theophylline[18] because of the absence of the electron-withdrawing groups. As with glycine, histidine only has a COO^- group and not a protonated carboxylic acid (COOH) group, hence the lower binding energy in comparison to aspartic and glutamic acid provides support for peak fitting the $COO^-$and COOH carbons as separate components (Figure 4, Table 2). The $\underline{C}-C$, $\underline{C}-N$, and COO^- C 1s photoemission lines of arginine occur at 285.0, 286.1, and 288.1 eV respectively, while the unusual carbon of the guanidinium group, with its three neighbouring nitrogen atoms and delocalized positive charge, is shifted to higher BE at 289.0 eV (Figure 4e, Table 3). The increased chemical shift for the highest binding energy peak compared to histidine confirms the separate peak components for the COO^- and guanidinium carbons (Figure 4c and d).

The overall envelopes of the peptide experimental C 1s spectra differ strongly (Figure 6). Comparison between the elemental compositions derived from XPS survey scans (Table 4) and those expected from stoichiometry clearly reveals an excess of oxygen and carbon relative to nitrogen, a small Si signal for RGD and RGDSC, and a fluorine signal for RGDSC, reflecting the difficulty involved in purifying peptides and the sensitivity of XPS to even minor impurities. The presence of fluorine for RGDSC indicates some residual

5

trifluoroacetic acid (TFA, CF_3CO_2H), commonly used to purify peptides or to cleave peptide from its support.[51,54,60] This is reflected in the atomic % values (Table 4) and a $\underline{C}-F_3$ component at 292.5 eV in the C 1s photoemission (Figure 5c), indicating a 1:1 molar ratio of RGDSC and TFA in the surface region probed by XPS, as well as some contribution around 289 eV from the carboxylic acid/carboxylate of TFA. Both RGD and RGDSC exhibit a Si signal in XPS, signifying a further impurity. The binding energy of the Si 2p signal around 102 eV is indicative of Si−O species, such as those found in siloxanes, Si(−R)O, where R is a hydrocarbon chain.[61] Siloxanes are a common trace impurity with organic compounds, usually at low enough bulk levels to be insignificant for bulk properties. However, they have a low solubility in the crystal bulk and therefore have a tendency to accumulate at the surface, resulting in a significant contribution to the photoemission.[61] The presence of siloxanes would increase the carbon and oxygen content, just as seen in the data (Table 4), particularly an enhanced $\underline{C}$−C component at 285 eV. The theoretically expected peak envelopes, constructed from the known compositions of the peptides (Figure 1, Table 2), are shown in Figure 5 (insets) alongside the peak-fitted peptide spectra (including the TFA contributions for RGDSC), demonstrating the strong impact of siloxane impurities particularly on the low-BE region of the C 1s data of RGD and RGDSC.

However, the elemental composition obtained by XPS for RGDS is quite close to the expected stoichiometric value (Table 4), showing that a quantitative fitting analysis of such tetrapeptide data can be carried out quite reliably. Prior knowledge of the expected chemical environments (Figure1, Table 2) and of the C 1s photoemission spectra of the amino acids allows the assignment of all peaks in the complex peptide spectrum. The expected peak components from $\underline{C}$−C, $\underline{C}$−COOH, $\underline{C}$−N/$\underline{C}$−NH$^+$, COO$^-$, and of the guanidinium carbon observed for the constituent amino acids can be fitted to the RGDS spectrum (Figure 5b, Table 3). Formation of the amide (peptide) bonds between the amino acid residues (Figure 1) results in increased contributions at 286.4 eV from $\underline{C}$−N and at 288.2 eV from O=$\underline{C}$−N (Table 3).

O 1s XPS

Glycine, histidine, and arginine exhibit only a single O 1s photoemission signal at 531.2-531.3 eV (Table 5, Figure 6a, d, e) confirming the carboxylate (COO$^-$) form. There is some asymmetry to high BE, which could arise from the occurrence of some differential surface charging, the presence of some adsorbed water/remaining solvent, contribution from residual COOH of malonic acid, or a naturally asymmetric lineshape.[52] The protonated carboxylic acid group (COOH) has two separate chemical environments for oxygen, $\underline{O}$=C−OH and O=C−$\underline{O}$H, occurring at BEs around 532 and 533 eV with a 1-1.5 eV BE shift between them.[55] The COO$^-$ in aspartic acid and glutamic acid arises at 531.5-531.6 eV, while the side-chain carboxylic acid group results in additional signals from the two carboxylic acid oxygen species: $\underline{O}$=C−OH occurs at 532.2-532.3 eV and O=C−$\underline{O}$H at 533.2-533.3 eV (Table 5, Figure 6b, c).

Peptide formation leads to the presence of amide oxygen centers ($\underline{O}$=C−N) and the loss of emission from carboxylic acid groups (Figure 1, Table 5). The C 1s analysis indicated that RGDS was the purest peptide sample. The O 1s signal of COO$^-$ of RGDS occurs at 531.2 eV and is accompanied by photoemission by the amide

(peptide bond) $\underline{O}$=C−N and the serine $\underline{O}$−H at 532.0 and 533.2 eV respectively (Figure 7b). Comparing with the O 1s emission from RGD reveals relatively small but significant intensity differences between the data (Figure 7a). As one would expect, the RGDS spectrum has somewhat more intensity in the region of the amide oxygen, but the O 1s emission from RGDSC is overall shifted to higher BE, which is difficult to explain by the addition of another amino acid to the sequence. It seems likely that the abovementioned impurities, which contain oxygen species, make O 1s peak fitting for RGD and RGDSC impracticable without knowledge of the types/amounts of Si-O species involved as well as the protonation state of the carboxyl group in TFA. The overall envelopes of the O 1s spectra are relatively similar for all three peptides (Figure 7a), illustrating that the O 1s emission is intrinsically less diagnostic and less specific than the C 1s and N 1s spectra, because of the relatively weaker chemical shifts for different oxygen environments.[55] Bulk hydration and/or water adsorption are likely additional contributors to the complexity of the O 1s data.

Conclusions

We have reported a set of C 1s, N 1s, and O 1s core level binding energies from a quantitative XPS analysis of several amino acids with different side-chain groups. As in our recent study of saccharides,[52] a contribution from adventitious hydrocarbon contamination is clearly evident for all samples, but can, due to its distinctive chemical shift, be quantitatively accounted for in the data analysis. For the γ-polymorph of glycine, a higher hydrocarbon contamination level may be associated with adsorbed additive (malonic acid) from the preparation process.

The imidazole group in histidine shows similar BE-shifted N centers as the photoemission from the two nitrogen centers in theophylline, although shifted to slightly lower BE values due to the absence of electron withdrawing groups. The observed BE shift between the two ring nitrogen species is also in good agreement with reported experimental values for aqueous imidazole solutions.[47,56] The unusual guanidinium chemical environment found in arginine is distinguished by nitrogen and carbon chemical shifts, with a high BE carbon photoemission.

With knowledge of the XPS data for the individual amino acids data we could interpret the photoemission data for RGD peptide systems. The zwitterionic nature of the amino acids and peptides in the solid state was clearly identifiable from the presence of signals from protonated amine and from carboxylate groups. The chemical shifts observed for the free amino acids assist characterization of the peptide RGDS, taking into account the formation of amide peptide bonds between the residues. We did find that XPS is very sensitive to common contaminants in peptide products (TFA, siloxanes), but the results for the comparatively pure tetrapeptide RGDS show that it is possible to detect the effect of adding another amino acid to the RGD sequence. In conclusion, XPS clearly has enough chemical sensitivity to distinguish between short oligopeptides sequences when amino acids with sufficiently distinctive side chains are involved, and when impurities do not obscure the data too strongly. Even though the C 1s and O 1s signals for RGD and RGDSC had strong contributions from impurities, variations in the N 1s intensities varied between these peptides were diagnostic, because the N 1s photoemission from additional amide groups was not obscured by the impurities.

Acknowledgements

References

[1]   U. Hersel, C. Dahmen, H. Kessler, Biomaterials**2003,** 23, 4385.

[2]   E. Ruoslahti, Annu.Rev.Cell Dev.Biol.**1996,** 12, 697.

[3]   J. H. Collier, T. Segura, Biomaterials**2011,** 32, 4198.

[4]   P. Schaffner, M. M. Dard, Cell.Mol.Life.Sci.**2003,** 60, 119.

[5]   S. E. D'Souza, M. H. Ginsberg, E. F. Plow, Trends.Biochem.Sci.**1991,** 16, 246.

[6]   F. Causa, E. Battista, R. Della Moglie, D. Guarnieri, M. Iannone, P. A. Netti, Langmuir**2010,** 26, 9875.

[7]   O. Drevelle, E. Bergeron, H. Senta, M. A. Lauzon, S. Roux, G. Grenier, N. Faucheux, Biomaterials**2010,** 31, 6468.

[8]   H. Sun, A. Wirsén, A.-C. Albertsson, Biomacromolecules**2004,** 5, 2275.

[9]   C. Battocchio, G. Iucci, M. Dettin, V. Carravetta, S. Monti, G. Polzonetti, Mater.Sci.Eng.B - Adv.**2010,** 169, 36.

[10]   P. G. Rouxhet, M. J. Genet, Surf.Interface Anal.**2011,** 43, 1453.

[11]   M. J. Genet, Ch. C. Dupont-Gillain, P. G. Rouxhet, in Medical Applications of Colloids, (Ed.: E. Matijevic), Springer:New York, **2008**, p. pp. 177-307.

[12]   Y. Y. Wang, L. X. Lu, J. C. Shi, H. F. Wang, Z. D. Xiao, N. P. Huang, Biomacromolecules**2011,** 12, 551.

[13]   A. C. de Luca, J. S. Stevens, S. L. M. Schroeder, J. P. Guilbaud, A. Saiani, S. Downes, G. Terenghi, J.Biomed.Mater.Res.A**2012,** Early view online (DOI:10.1002/jbm.a.34345).

[14]   C. L. Yang, K. Cheng, W. J. Weng, C. Y. Yang, J.Mater.Sci.- Mater.M.**2009,** 20, 2349.

[15]   M. C. Porté-Durrieu, C. Labrugère, F. Villars, F. Lefebvre, S. Dutoya, A. Guette, L. Bordenave, C. Baquey, J.Biomed.Mater.Res.**1999,** 46, 368.

[16]   Z. P. Zhang, R. Yoo, M. Wells, T. Beebe, R. Biran, P. Resco, Biomaterials**2005,** 26, 47.

[17]   D. T. Clark, J. Peeling, L. Colling, Biochim.Biophys.Acta**1976,** 453, 533.

[18]   J. S. Stevens, S. J. Byard, S. L. M. Schroeder, Cryst.Growth Des.**2010,** 10, 1435.

[19] J. S. Stevens, S. J. Byard, S. L. M. Schroeder, J.Pharm.Sci.**2010,** 99, 4453.

[20] J. S. Stevens, S. J. Byard, C. C. Seaton, G. Sadiq, R. J. Davey, S. L. M. Schroeder, Angew.Chemie - Int.Ed.**2011,** 50, 9916.

[21] J. S. Stevens, S. J. Byard, E. Zlotnikov, S. L. M. Schroeder, J.Pharm.Sci.**2011,** 100, 942.

[22] J. S. Stevens, S. J. Byard, C. A. Muryn, S. L. M. Schroeder, J.Phys.Chem.B**2010,** 114, 13961.

[23] P. G. Jönsson, A. Kvick, Acta Cystall.B - Stru.**1972,** B 28, 1827.

[24] R. E. Marsh, Acta Cryst.**1958,** 11, 654.

[25] Y. Iitaka, Acta Cryst.**1961,** 14, 1.

[26] L. J. W. Shimon, M. Lahav, L. Leiserowitz, Nouv.J.Chim.**1986,** 10, 723.

[27] J. L. Derissen, H. J. Endeman, A. F. Peerdema, Acta Cystall.B - Stru.**1968,** B 24, 1349.

[28] N. Hirayama, K. Shirahata, Y. Ohashi, Y. Sasada, Bull.Chem.Soc.Jap.**1980,** 53, 30.

[29] J. J. Madden, N. C. Seeman, E. L. McGandy, Acta Cystall.B - Stru.**1972,** 28, 2377.

[30] J. J. Madden, E. L. McGandy, N. C. Seeman, Acta Cystall.B - Stru.**1972,** 28, 2382.

[31] M. S. Lehmann, T. F. Koetzle, W. C. Hamilton, Int.J.Pept.Prot.Res.**1972,** 4, 229.

[32] M. S. Lehmann, J. J. Verbist, W. C. Hamilton, T. F. Koetzle, J.Chem.Soc.Perk.T.2**1973,** 133.

[33] D. Nolting, E. F. Aziz, N. Ottosson, M. Faubel, I. V. Hertel, B. Winter, J.Am.Chem.Soc.**2007,** 129, 14068.

[34] M. J. Bozack, Y. Zhou, S. D. Worley, J.Chem.Phys.**1994,** 100, 8392.

[35] K. Uvdal, P. Bodö, A. Ihs, B. Liedberg, W. R. Salaneck, J.Colloid Interf.Sci.**1990,** 140, 207.

[36] A. Chatterjee, L. Y. Zhao, L. Zhang, D. Pradhan, X. J. Zhou, K. T. Leung, J.Chem.Phys.**2008,** 129.

[37] K. Siegbahn, C. Nordling, A. Fahlman, R. Nordberg, K. Hamrin, J. Hedman, G. Johansson, T. Bergmark, S.-E. Karlsson, I. Lindgren, B. Lindberg, ESCA. Atomic, Molecular and Solid State Structure Studied by means of Electron Spectroscopy (Nova Acta Regiae Societatis Scientiarum Upsaliensis, Ser.IV Vol.20), Almqvist & Wiksells Boktryckeri AB:Uppsala, **1967**.

[38] K. L. Cheng, J. W. Prather II., T. A. Carlson, CRC Critical Reviews in Analytical Chemistry**1975,** 5, 37.

[39] K. D. Bomben, S. B. Dev, Anal.Chem.**1988,** 60, 1393.

[40] W. Zhang, V. Carravetta, O. Plekan, V. Feyer, R. Richter, M. Coreno, K. C. Prince, J.Chem.Phys.**2009,** 131, 035103.

[41] V. Feyer, O. Plekan, R. Richter, M. Coreno, K. C. Prince, V. Carravetta, J.Phys.Chem.A**2009,** 113, 10726.

[42]   V. Feyer, O. Plekan, R. Richter, M. Coreno, K. C. Prince, V. Carravetta, J.Phys.Chem.A**2008,** 112, 7806.

[43]   V. Feyer, O. Plekan, R. Richter, M. Coreno, K. C. Prince, V. Carravetta, M. de Simone, J.Phys.Chem.A**2007,** 111, 10998.

[44]   O. Plekan, V. Feyer, R. Richter, M. Coreno, M. de Simone, K. C. Prince, V. Carravetta, Chem.Phys.Lett.**2007,** 442, 429.

[45]   O. Plekan, V. Feyer, R. Richter, M. Coreno, M. de Simone, K. Prince, V. Carravetta, J.Electron Spectrosc.Relat.Phenom.**2007,** 156, LXVIII.

[46]   O. Plekan, V. Feyer, R. Richter, M. Coreno, M. de Simone, K. Prince, V. Carravetta, J.Electron Spectrosc.Relat.Phenom.**2007,** 155, 47.

[47]   D. Nolting, N. Ottosson, M. Faubel, I. V. Hertel, B. Winter, J.Am.Chem.Soc.**2008,** 130, 8150.

[48]   B. Jagoda-Cwiklik, P. Slavícek, D. Nolting, B. Winter, P. Jungwirth, J.Phys.Chem.B**2008,** 112, 7355.

[49]   B. Jagoda-Cwiklik, P. Slavícek, L. Cwiklik, D. Nolting, B. Winter, P. Jungwirth, J.Phys.Chem.A**2008,** 112, 3499.

[50]   M. Thomason, G. Hembury, E. F. Aziz, C. R. Seabourne, A. J. Scott, S. L. M. Schroeder, Phys.Chem.Chem.Phys.**2012,** in preparation.

[51]   RGD (Arg-Gly-Asp) specification sheet, Sigma-Aldrich Co. LLC., **2012**.

[52]   J. S. Stevens, S. L. M. Schroeder, Surf.Interface Anal.**2009,** 41, 453.

[53]   N. Fairley, A. Carrick, The CASA Cookbook: Recipes for XPS Data Processing, pt. 1, Acolyte Science:Knutsford, Cheshire, **2005**.

[54]   D. Briggs, M. P. Seah, P. M. A. Sherwood, in P*ractical Surface Analysis, Volume 1: Auger and X-ray Photoelectron Spectroscopy*, (Eds.: D. Briggs, M. P. Seah), Wiley:Chichester, **1990**.

[55]   The XPS of Polymers Database, 1 ed. (Eds.: G. Beamson, D. Briggs) Surface Spectra Ltd:Manchester, UK, **2000**.

[56]   G. Xue, Q. Dai, S. Jiang, J.Am.Chem.Soc.**1988,** 110, 2393.

[57]   D. S. Eggleston, S. H. Feldman, Int.J.Pept.Prot.Res.**1990,** 36, 161.

[58]   M. R. Alexander, G. Beamson, C. J. Blomfield, G. Leggett, T. M. Duc, J.Electron Spectrosc.Relat.Phenom.**2001,** 121, 19.

[59]   D. Briggs, D. M. Brewis, R. H. Dahm, I. W. Fletcher, Surf.Interface Anal.**2003,** 35, 156.

[60]   P. Wadhwani, E. Strandberg, in Fluorine in Medicinal Chemistry and Chemical Biology, (Ed.: I. Ojima), Wiley-VCH:Weinheim, **2009**, p. pp. 463-493.

[61]   M. A. Reijme, A. W. D. van der Gon, M. Draxler, A. Gildenpfennig, F. J. J. Janssen, H. H. Brongersma, Surf.Interface Anal.**2004,** 36, 1.

Table 1.XPS N 1s peak assignments, binding energies, and emission intensity ratios.

Amino acid / peptide	Binding energy / eV					Emission intensity ratio	
	N=C−NH	C−N	N=C−NH	O=C−N / guanidinium $H_2N-C(=NH_2^+)-NH-CH_3$	C−NH$^+$	Found	Expected
α-glycine					401.4	1	1
γ-glycine					401.4	1	1
Aspartic acid					401.6	1	1
Glutamic acid					401.5	1	1
Histidine	398.8		400.4		401.4	0.9:1:0.9	1:1:1
Arginine		399.2		400.0		1:2.9	1:3
RGD				400.1	401.6	5.5:1	5:1
RGDS				400.2	401.5	6:1	6:1
RGDSC				400.2	401.7	6.6:1	7:1

Table 2. Number of types of carbon chemical environment per chemical structure.

Amino acid / peptide	Number of types of chemical environment per molecule							
	$\underline{C}$–C / $\underline{C}$-S	$\underline{C}$–COO	C=$\underline{C}$–N	$\underline{C}$–N / C–$\underline{N}$H$^+$ / $\underline{C}$–O	N=$\underline{C}$–NH	O=$\underline{C}$–N / $\underline{C}$OO$^-$		$\underline{C}$OOH
Average BE/eV	285.0	285.4	285.6	286.35	286.7	288.35	289.2	289.3
α-glycine	0			1		1		
γ-glycine	0			1		1		
Aspartic acid	0	1		1		1		1
Glutamic acid	1	1		1		1		1
Histidine	1		2	1	1	1		
Arginine	2			2		1	1	
RGD	2	1		4		4	1	
RGDS	2	1		6		5	1	
RGDSC	3	1		7		6	1	

Table 3. XPS C 1s peak assignments and binding energy positions.

Amino acid / peptide	Binding energy / eV							
	$\underline{C}$–C / $\underline{C}$-S	$\underline{C}$–COO	C=$\underline{C}$–N	$\underline{C}$–N C–$\underline{N}$H$^+$ / $\underline{C}$–O	/ N=$\underline{C}$–NH	O=$\underline{C}$–N / $\underline{C}$OO$^-$	guanidinium	$\underline{C}$OOH
α-glycine	285.0			286.4		288.5		
γ-glycine	285.0			286.3		288.4		
Aspartic acid	285.0	285.4		286.6		288.5		289.4
Glutamic acid	285.0	285.4		286.4		288.4		289.2
Histidine	285.0		285.6	286.2	286.7	288.3		
Arginine	285.0			286.1		288.1	289.0	
RGD	285.0	285.4		286.4		288.3	289.2	
RGDS	285.0	285.4		286.4		288.2	289.3	
RGDSC	285.0	285.4		286.5		288.5	289.3	

Table 4. XPS elemental compositions (atomic %), and those corrected for adventitious hydrocarbon contamination[52] (values expected from molecular formula in italics).

Amino acid / peptide	XPS experimental values						Minus hydrocarbon contamination				
	C %	O %	N %	S %	F %	Si %	C %	O %	N %	S%	Si%
α-Glycine	50.9	32.4	16.7	/	/	/	41.7	38.5	19.8	/	/
							40	*40*	*20*		
γ-Glycine	50.5	33.3	16.2	/	/	/	38.7	41.3	20.0	/	/
							40	*40*	*20*		
Aspartic acid	55.6	35.5	8.9	/	/	/	44.6	44.3	11.1	/	/
							44.4	*44.4*	*11.1*		
Glutamic acid	59.9	31.5	8.6	/	/	/	48.7	40.3	11.0	/	/
							50	*40*	*10*		
Histidine*	62.4	16.2	21.4	/	/	/	50.5	21.4	28.1	/	/
							54.5	*18.2*	*27.3*		
Arginine	59.4	14.4	26.2	/	/	/	49.9	17.8	32.3	/	/
							50	*16.7*	*33.3*		
RGD†	69.5	18.6	9.6	/	/	2.3	63.2	22.5	11.6	/	2.7
							50	*25*	*25*		*0*
RGDS	57.5	23.1	19.4	/	/	/	52.5	25.8	21.7	/	/
							50	*26.7*	*23.3*		
RGDSC†‡	66.7	19.6	9.1	1.2	/	3.4	60.0	22.9	10.7	1.4	4.0
[original]	63.6	20.3	8.4	1.1	3.5	3.1	*50*	*25*	*22.2*	*2.8*	*0*

*A similar value as for the other amino acids was assumed in the subtraction of the adventitious carbon contribution.

† Some F from TFA contributes to increased C and O levels. The TFA contribution was removed based on the F %.

‡A similar value as for RGDS was assumed in the subtraction of the adventitious carbon contribution due to the Si-containing impurity contributing to increased C and O levels.

Table 5.XPS O 1s peak assignments and positions.

Amino acid / peptide	Binding energy / eV					Peak area ratios	
	COO⁻	O=C–N	O=C–O	C–OH	O=C–O	Found	Expected
α-glycine	531.3					1	1
γ-glycine	531.2					1	1
Aspartic acid	531.5		532.3		533.3	2.1:1.1:1	2:1:1
Glutamic acid	531.6		532.2		533.2	2.4:1.3:1	2:1:1
Histidine	531.3					1	1
Arginine	531.2					1	1
RGD	*	*				/	4:2
RGDS	531.2	532.0		533.2		4:3:1	4:3:1
RGDSC	*	*		*		/	4:4:1

*Expected chemical environments from the peptide (not fit).
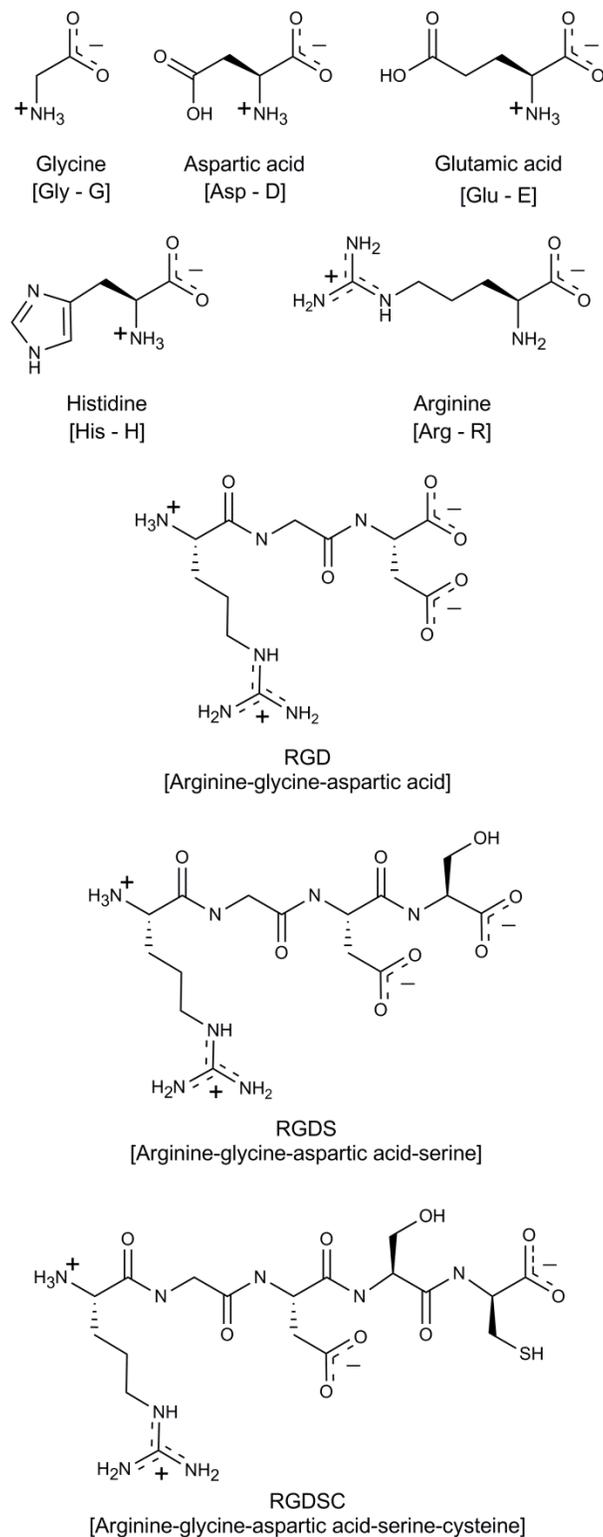
Figure 1. Chemical structures of the zwitterionic forms of the amino acids and the three peptides investigated in this study.
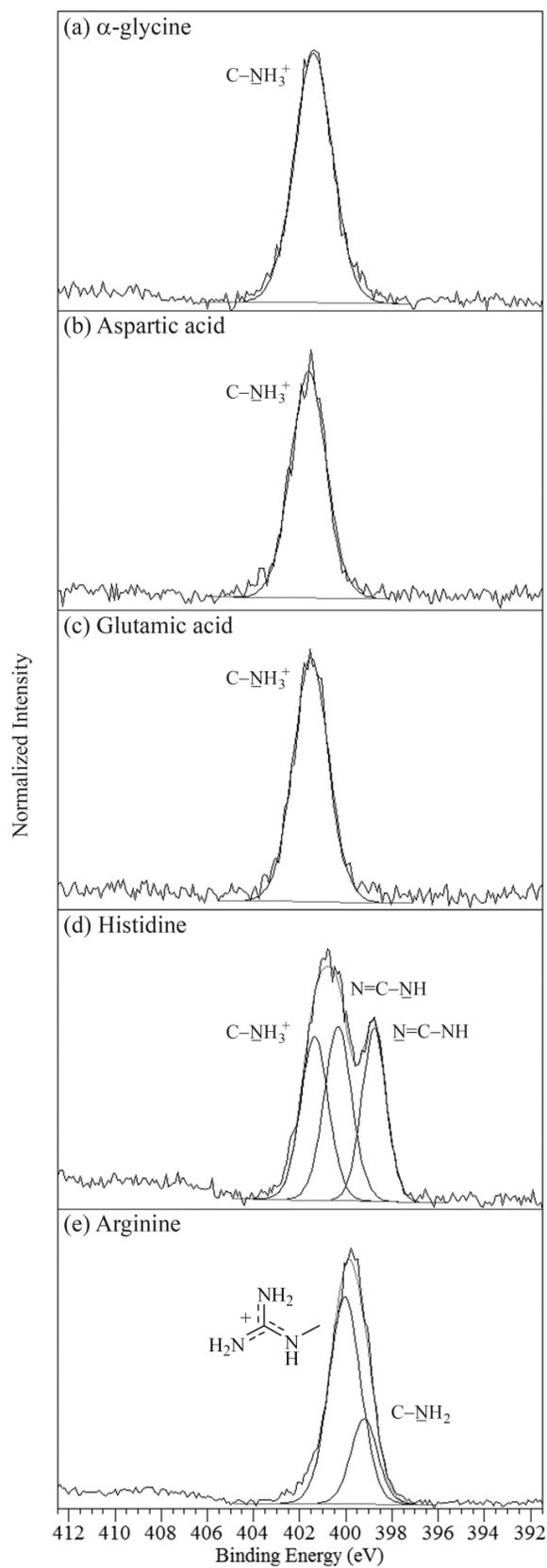
Figure 2. XPS N 1s spectra of the amino acids: (a) α-glycine, (b) aspartic acid, (c) glutamic acid, (d) histidine, and (e) arginine.
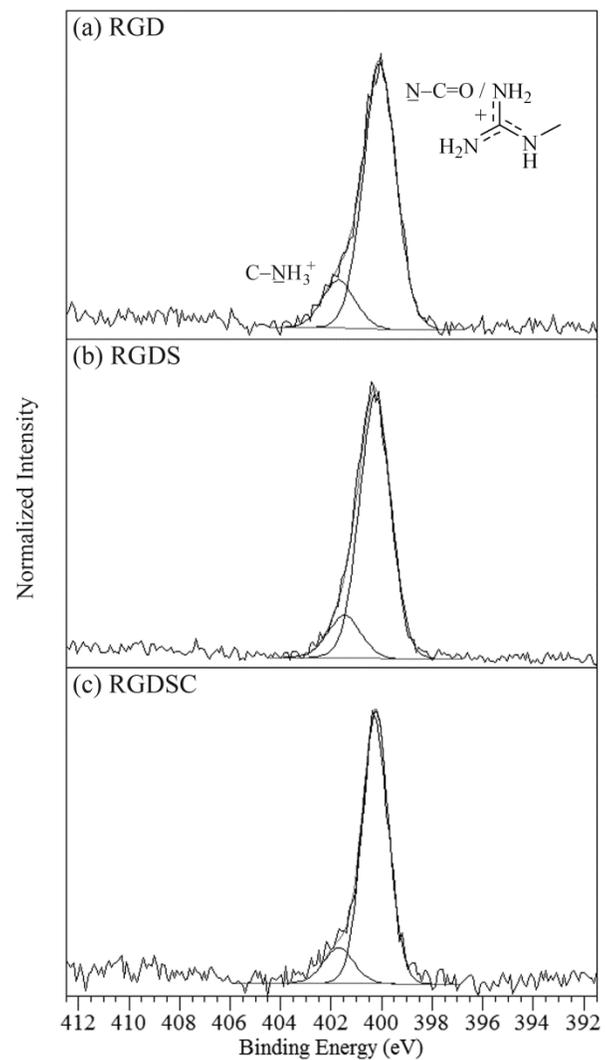
**Figure 3.** XPS N 1s spectra of peptides: (a) RGD, (b) RGDS, and (c) RGDSC.
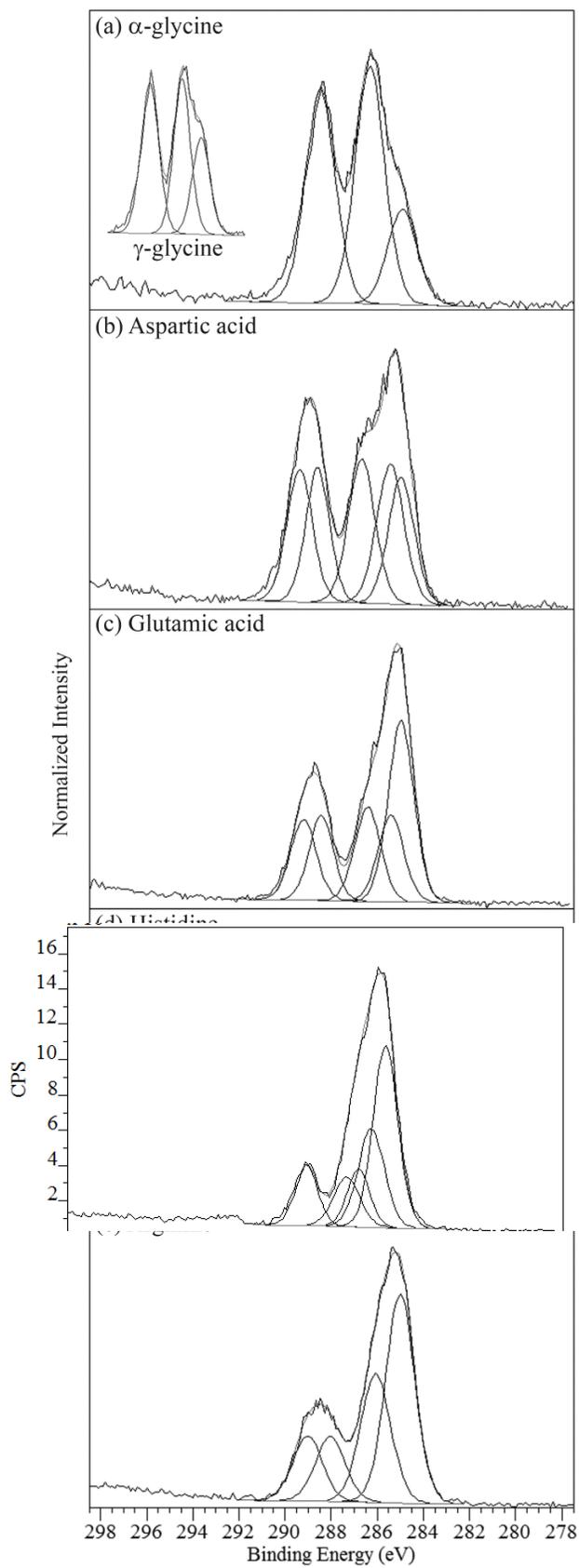
Figure 4. XPS C 1s spectra of the amino acids: (a) α-glycine (inset γ-glycine), (b) aspartic acid, (c) glutamic acid, (d) histidine, and (e) arginine.
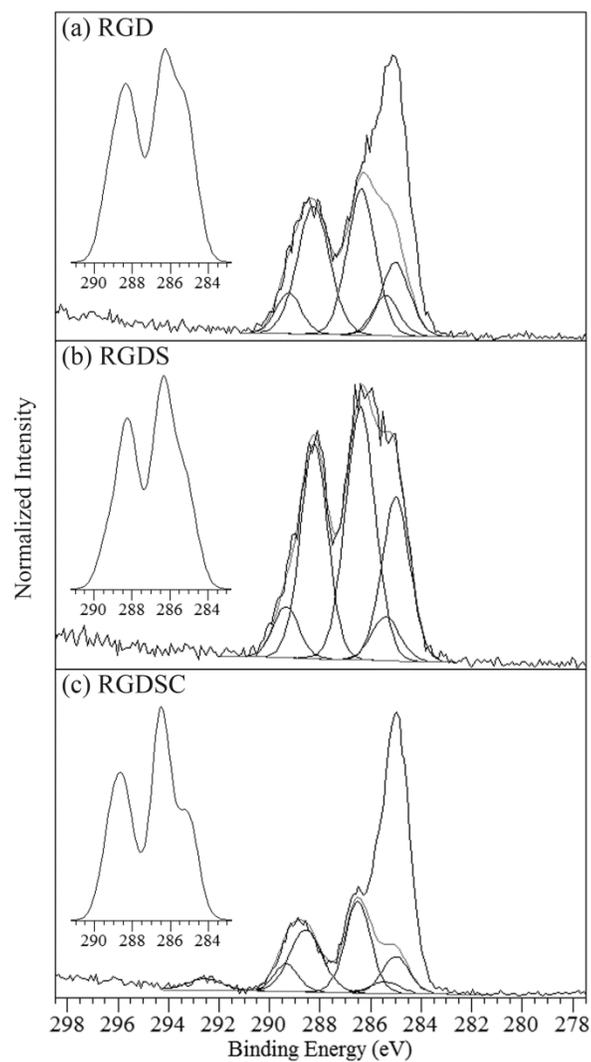
Figure 5. XPS C 1s spectra of peptides: (a) RGD, (b) RGDS, and (c) RGDSC, with the stoichiometric peak components shown for RGD and RGDSC+TFA, and the expected peak shape for all three peptides in the absence of impurities/contamination.
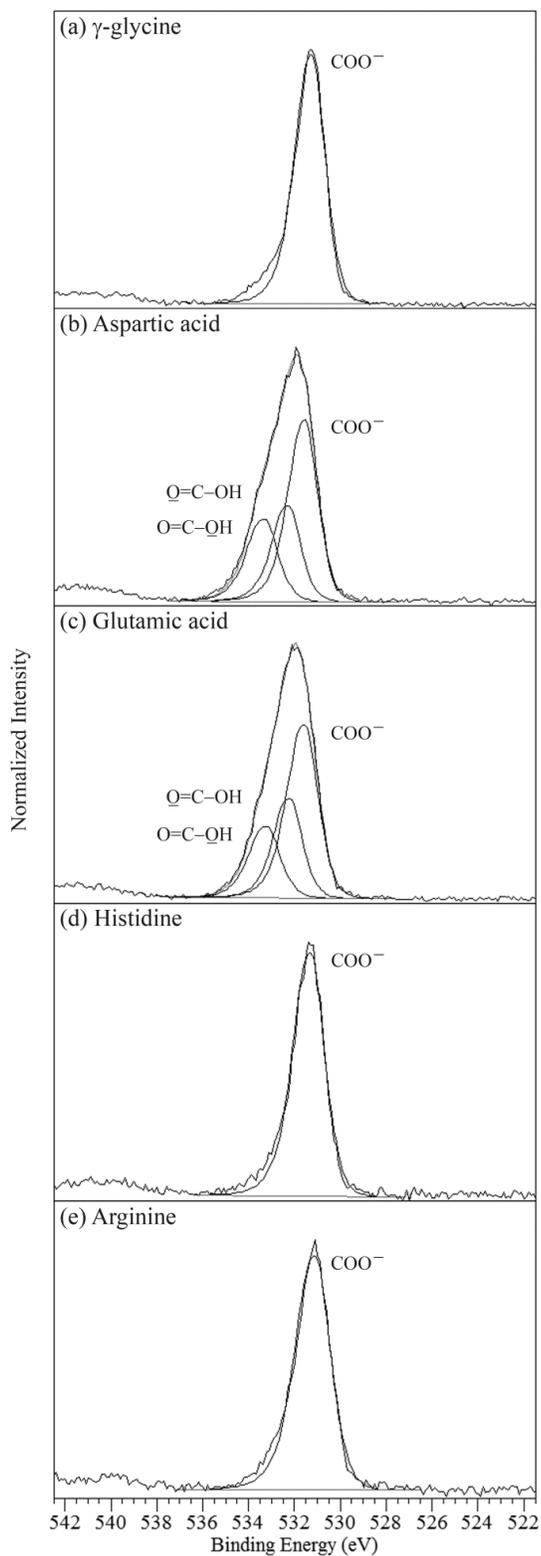
Figure 6. XPS O 1s spectra of the amino acids: (a) α-glycine (b) aspartic acid, (c) glutamic acid, (d) histidine, and (e) arginine.
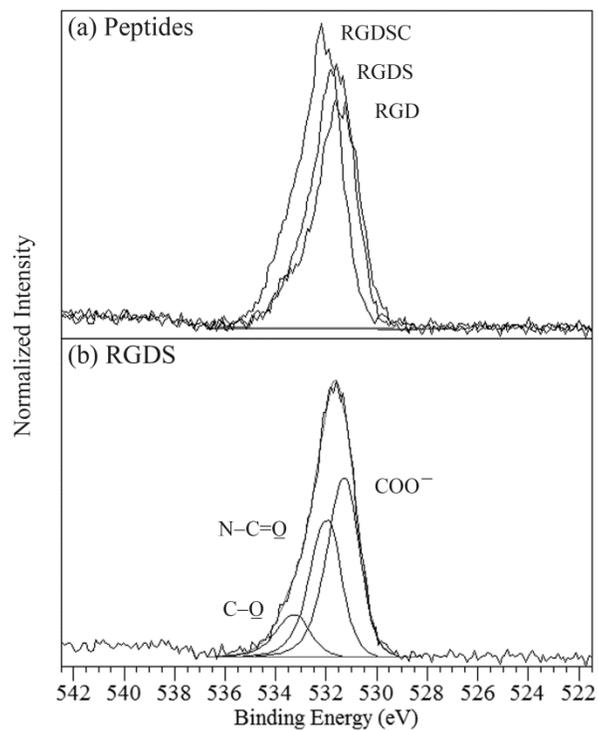
Figure 7. XPS O 1s spectra of (a) all three peptides, showing the similarity in peak shape and (b) peak fitting for RGDS.